

Calculated neutron diffraction peak intensities for the present structure are also listed in Table 2, together with experimental values of Wang *et al.* (1972). The negative atomic scattering factor for Ti accentuates the superlattice peaks of the TiNi martensite. There is reasonable matching of the major peaks with those calculated from the present structure. The absence of any observed intensity for the 4.12 Å *d*-spacing reflection from both X-ray and neutron diffraction serves as evidence that the *c* axis of the present structure is indeed the unique axis. The final point supporting the present structure concerns the Ti–Ti bond lengths generated from the final atom positions. The values of around 2.9 Å are consistent with those observed in all the other structures in the Ti–Ni system.

### References

- DAUTOVICH, D. P. & PURDY, G. R. (1965). *Can. Metall. Q.* **4**, 129–143.
- GUPTA, S. P. (1972). *Martensitic Transformation and Stacking Modulations in Titanium–Nickel Alloys of Near-Equiatomic Composition*. PhD Thesis, Polytechnic Institute of Brooklyn.
- GUPTA, S. P. & JOHNSON, A. A. (1973). *Trans. Jpn Inst. Met.* **14**, 292–302.
- GUPTA, S. P., JOHNSON, A. A. & MUKHERJEE, K. (1973). *Mater. Sci. Eng.* **11**, 29–41.
- HEHEMANN, R. F. & SANDROCK, G. D. (1971). *Scr. Metall.* **5**, 801–806.
- International Tables for X-ray Crystallography* (1968). Vol. III. Birmingham: Kynoch Press.
- LARSON, D. J. (1979). *The Physical and Mechanical Properties of Near Equiatomic TiNi*. PhD Thesis, Northwestern Univ.
- MARCINKOWSKI, M. J., SASTRI, A. S. & KOSKIMAKI, D. (1968). *Philos. Mag.* **18**, 945–958.
- MICHAL, G. M. (1979). *Diffusionless Transformations in TiNi*. PhD Thesis, Stanford Univ.
- MOHAMED, H. A. (1976). *Martensitic Transformation and Shape Memory Effect in Ni–Ti Alloy*. PhD Thesis, Univ. of California at Berkeley.
- MOHAMED, H. A. & WASHBURN, J. (1977). *J. Mater. Sci.* **12**, 469–480.
- NAGASAWA, A. (1971). *J. Phys. Soc. Jpn*, **31**, 136–147.
- ÖLANDER, A. (1932). *Z. Kristallogr.* **83A**, 145–149.
- OTSUKA, K., SAWAMURA, T. & SHIMIZU, T. (1971). *Phys. Status Solidi A*, **5**, 457–470.
- SANDROCK, G. D. (1971). *Diffusionless Phase Transitions in Near-Equiatomic Intermetallic Compound Titanium–Nickel*. PhD Thesis, Case Western Reserve Univ.
- VATANAYON, S. & HEHEMANN, R. F. (1975). *Shape Memory Effects in Alloys*, edited by A. J. PERKINS, pp. 115–146. New York: Plenum Press.
- WANG, F. E., PICKART, S. J. & ALPERIN, H. A. (1972). *J. Appl. Phys.* **43**, 97–112.
- ZENER, C. (1947). *Phys. Rev.* **71**, 846–851.

*Acta Cryst.* (1981). **B37**, 1807–1812

## The Structure and Polytypism of the $\beta$ Modification of Copper(I) Thiocyanate\*

BY DOUGLAS L. SMITH AND VERNON I. SAUNDERS

Research Laboratories, Eastman Kodak Company, Rochester, New York 14650, USA

(Received 5 January 1981; accepted 9 March 1981)

### Abstract

Crystals of  $\beta$ -CuNCS grow as trigonal pyramids. The crystals consist of  $3R$  and  $2H$  polytypes in syntactic coalescence along with some disorder and twinning. The space groups are  $R3m$  and  $P6_3mc$ . The lattices have  $a = 3.856$  (1) Å. For the  $3R$  form,  $c = 16.453$  (2) Å, and for  $2H$ ,  $c = 10.97$  Å. The structures are composed of (001) layers of closest-packed cylinders of CuNCS units. As in the case of spheres, there are three possible layer positions called *A*, *B*, and *C* in the *xy* plane. Adjacent layers are bonded to each other by strong Cu–S bonds [2.343 (1) Å] such that

both Cu and S are tetrahedrally coordinated and the crystal is a three-dimensional polymer. The structure was solved by inspection and refined to  $R = 0.016$  for a strong subset (67 reflections) of the data. Refinement of scale factors for other subsets of the data showed the crystal to be 87% *ABC*, 1% *ACB*, 3% *AB*, and 9% disordered or other polytypes.

### Introduction

The reduction of  $\text{Cu}^{\text{II}}$  salts in the presence of thiocyanate ions under various conditions yields at least two polymorphic forms of copper(I) thiocyanate (Kruger, Bussem & Tschirch, 1936; Kruger &

\* Alternative name: *poly- $\mu$ -(thiocyanato-*N,S*)-copper(I)*.

Tschirch, 1941; Garaj & Gazo, 1965) which have been well characterized by their X-ray powder diffraction patterns (JCPDS, 1979). The single-crystal structure of  $\alpha$ -CuNCS, the orthorhombic form, has been reported recently (Kabesova, Dunaj-Jurco, Serator, Gazo & Garaj, 1976). We report here the preparation and crystal structure of  $\beta$ -CuNCS, the crystals of which comprise  $3R$  and  $2H$  polytypes in syntactic coalescence.

## Experimental

### 1. Preparation

Polymorphic forms of CuNCS were originally reported by Kruger, Bussem & Tschirch (1936) and by Kruger & Tschirch (1941). They prepared the  $\beta$  form, which they designated type (a), by slow precipitation from a solution of  $\text{CuSO}_4$  and KNCS and the  $\alpha$  form, type (b), from an acidified solution of  $\text{Cu}(\text{NCS})_2$  to which  $\text{Na}_2\text{S}_2\text{O}_3$  had been added. Both forms were reported to be white in the absence of iodide; crystals of type (a) were trigonal pyramidal and of type (b) were chunky in habit. Distinct X-ray powder diffraction patterns were reported for each form.

Recently, Garaj & Gazo (1965) and Kabesova, Dunaj-Jurco, Serator, Gazo & Garaj (1976) have prepared  $\alpha$ - and  $\beta$ -CuNCS by the slow reduction of  $\text{Cu}(\text{NH}_3)_2(\text{NCS})_2$  formed in solutions containing  $\text{CuSO}_4$ ,  $\text{NH}_4\text{NCS}$ ,  $\text{NH}_4\text{OH}$ , and  $(\text{NH}_4)_2\text{CO}_3$ . The  $\beta$  compound was reported to be brown and the  $\alpha$ , white. Relatively large crystals of  $\alpha$ -CuNCS were obtained, and its crystal structure was determined (Kabesova, Dunaj-Jurco, Serator, Gazo & Garaj, 1976). By these techniques, we have not been successful in obtaining crystals of  $\beta$ -CuNCS free of  $\alpha$ -CuNCS, nor have we obtained crystals large enough for crystal structure analysis.

We have grown large crystals of both  $\alpha$ - and  $\beta$ -CuNCS by slow vapor dilution of aqueous solutions of CuNCS in NaNCS. Finely divided CuNCS was mixed with concentrated NaNCS (2.5–8 M) until there appeared to be a small excess of CuNCS. Diatomite filter aid was then stirred in, and the mixture was filtered into an evaporating dish. This was set on a perforated disk above a supply of water in a closed desiccator. Because of the photosensitivity of cuprous salts, the vessel was kept dark, and solutions and products were examined only in yellow light. Over periods of 3 to 6 weeks, chunky crystals, plates, bars, or needles were produced, depending upon the initial concentration of NaNCS. These were characterized as  $\alpha$ -CuNCS by X-ray powder diffraction (JCPDS, 1979) and by the CN stretching frequency in the infrared spectrum. In the course of our studies, a CN absorption band at  $2157\text{ cm}^{-1}$  has been correlated with  $\alpha$ -CuNCS; a band at  $2173\text{ cm}^{-1}$  arises from  $\beta$ -CuNCS. These

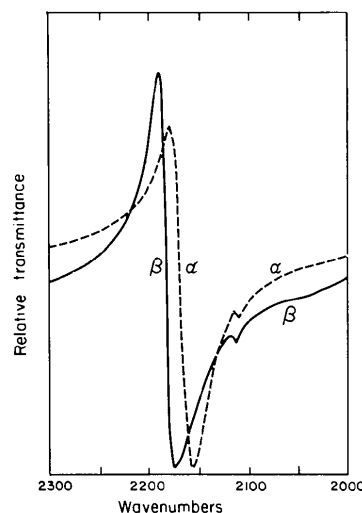


Fig. 1. Infrared absorption for CN stretch of  $\alpha$ - and  $\beta$ -CuNCS in KBr pellets. The transmittance spikes at  $2180$ – $2190\text{ cm}^{-1}$  are a consequence of the Christiansen effect and are dependent on the indices of refraction and fineness of division of the two materials in the pellet.

bands are illustrated in Fig. 1 and are consistent with those reported at  $2159$  and  $2173\text{ cm}^{-1}$  by Tramer (1962) and at  $2173\text{ cm}^{-1}$  by Kabesova, Kohout & Gazo (1978) for CuNCS of unknown phase.

With this procedure, we obtained from the most dilute solution studied crystals whose IR spectrum indicated a mixture of  $\alpha$ - and  $\beta$ -CuNCS. These consisted of needles up to 1 mm and conical crystals up to  $0.05\text{ mm}$  long.

Pure  $\beta$ -CuNCS was obtained by introducing ammonia to the CuNCS/NaNCS solutions by means of a second vessel containing a solution of  $1\text{ M}$   $(\text{NH}_4)_2\text{CO}_3$ . In this way a copper ammine thiocyanate complex is formed, which renders the solution green. From a solution of  $\sim 3\text{ M}$  NaNCS, small conical crystals formed in 6 days, and after 2 weeks the crystals were large enough ( $\sim 0.2\text{ mm}$ ) to be suitable for X-ray structure work. By IR (peak at  $2175\text{ cm}^{-1}$ ) these were identified as pure  $\beta$ -CuNCS. A few clusters of a blue copper ammonium complex that had also formed were easily separated from the colorless CuNCS. Applying this method to a solution of  $\sim 6\text{ M}$  NaNCS, we first obtained convex lens-shaped  $\alpha$ -CuNCS crystals. However, after the source of the ammonia was removed and the water was replaced in the desiccator, as the ammonia left the crystallization vessel, the crops of crystals harvested changed from  $\alpha$ - to  $\beta$ -CuNCS.

Pure crystals of both  $\alpha$ - and  $\beta$ -CuNCS are practically colorless. The  $\alpha$  form occurs in a variety of crystal habits. Particularly well formed crystals of  $\alpha$ -CuNCS up to  $0.5\text{ mm}$  have been obtained in 3 weeks by allowing our initial CuNCS–NaNCS solution to diffuse into silica gel. The  $\beta$  form always occurs as conical crystals with either a trigonal or a hexagonal base, *i.e.*

either as  $3m$  or as  $6mm$  morphology, and are readily recognized.

## 2. X-ray measurements

In the course of this study, two trigonal-pyramidal crystals, approximately 0.09 mm along the base and 0.17 mm high, were investigated both on an Enraf-Nonius CAD-4 diffractometer and by precession photographs. Lattice constants had been reported by JCPDS (1979) to be  $a = 3.857$  and  $c = 16.449$  Å with space group  $R3m$  and  $Z = 3$ . An initial automatic cell search on the CAD-4 yielded a cell of twice the volume with  $a = 3.856$  (1) and  $c = 32.922$  (13) Å. A check of reflections equivalent in spacing to 212 showed the crystal to be trigonal with  $\bar{3}m$  as the Laue group. A rapid data set collected for  $2\theta < 50^\circ$  (Mo  $K\alpha$ ) for all  $h \geq 0$ ,  $k \geq h$ ,  $\pm l$  showed the intensities to be strong for reflections corresponding to an  $R$ -centered cell with  $c = 16.46$  Å, medium for reflections with  $h - k \neq 3n$ ,  $l = 3n$ , and very weak or absent for the rest.

Precession photographs of the first crystal verified the Laue group and the intensity distribution of the diffractometer data and, in addition, showed faint streaking along reciprocal-lattice rows parallel to  $c^*$ . Precession photographs of a second crystal exhibited the same pattern of strong spots and very weak streaks. However, the reflections with  $h - k \neq 3n$ ,  $l = 3n$  were relatively much weaker than before and, in addition, new very weak spots occurred for  $h - k + l/2 = 3n$  which correspond to the *reverse* orientation or  $60^\circ$  twin of the strong cell. These observations indicated that the crystals are a coalescence of at least two forms and contain disorder and twinning as well.

Because the second crystal appeared to contain considerably less of the weakly diffracting components than the first one, it was mounted on the diffractometer for data collection. Least-squares refinement of 16 carefully centered reflections gave  $a = 3.856$  (1) and  $c = 32.905$  (4) Å. Intensities were measured at  $297 \pm 1$  K for  $h \geq 0$ ,  $k \geq h$ ,  $\pm l$  with graphite-monochromated Mo  $K\alpha$  radiation by the  $\omega$ - $2\theta$  scan technique ( $2\theta < 70^\circ$ ) from  $2\theta(\text{Mo } K\alpha_1) - 0.6^\circ$  to  $2\theta(\text{Mo } K\alpha_2) + 0.6^\circ$ . The scan rate was adjusted between 1 and  $20^\circ \text{ min}^{-1}$  ( $2\theta$ ) so that the significant intensities had  $\sigma(I)/I = 0.02$ . Backgrounds were measured by extending the scan range 25% at each end. The intensities of three standard reflections, remeasured after every 2500 s of X-ray exposure, showed no significant variations. Neither crystal investigated showed any sign of decomposition in the X-ray beam or in room light.

Intensities were calculated according to  $I = AS(C - RB)$ , where  $A$  is the attenuator factor,  $S$  is the scan rate,  $C$  is the total integrated peak count,  $B$  is the total background count, and  $R$  is the ratio of peak time to background time. Standard deviations were calculated according to  $\sigma^2(I) = (AS)^2(C + R^2B)$  and  $\sigma(F_o) =$

$\{[I + \sigma(I)]/Lp\}^{1/2} - F_o$  where  $(Lp)^{-1}$  is the Lorentz-polarization correction and  $F_o = (I/Lp)^{1/2}$  is the observed structure factor. An empirical absorption correction [ $\mu(\text{Mo } K\alpha) = 8.4 \text{ mm}^{-1}$ ] based on  $\psi$  scans (North, Phillips & Mathews, 1968) was made for which the normalized correction factor for  $I$  ranged from 0.69 to 1.00. The total number of reflections measured was 974, of which 103 represented redundant (in  $R3m$ )  $hkl$  reflections. Only 357 reflections exceeded  $\sigma(I)$ .

The entire data set was separated into six subsets based on intensities and combinations of indices. The number of reflections in each subset as well as the number with  $I > \sigma(I)$  and the maximum value of  $F_o$  are given in Table 1. The reflections of subsets 1 and 2 are very intense and account for almost all of the ordered Bragg scattering. The intensities in subsets 3 and 4 are much weaker, being only about 1% and 3%, respectively, of subset 2, but they are significant with more than 40% of the reflections being greater than  $\sigma(I)$  and values of  $F_o$  as high as  $108\sigma(F_o)$ . Intensities in subsets 5 and 6 are extremely weak; less than 20% are greater than  $\sigma(I)$  and these two classes were considered as 'unobserved'.

The indices of subsets 1 and 2 together describe an  $R$ -centered cell with  $c' = c/2 = 16.453$  (2) Å. As will be shown below, this cell is a  $3R$  polytype, which is also designated  $ABC$  to specify the stacking sequence of the layers of the structure. For subset 3, the  $hkl$  structure factors equal about 10% of the corresponding  $hkl$  structure factors of subset 2. Therefore, the indices of subsets 1 and 3 together correspond to the *reverse* setting of the strong  $R$  cell described by subsets 1 and 2. This cell can be designated by the layer sequence  $ACB$ . The reflections of subset 4, together with those of subset 1, describe a  $2H$  polytype, designated  $AB$ , with  $c' = c/3 = 10.97$  Å. Intensities in subset 5 could arise from higher-order polytypes such as  $6H$ , but the few significant reflections in this subset are probably measurements of the disorder streaking. The reflections of subset 6 should be systematically absent for all polytypes, including disordered regions. Therefore, subsets 5 and 6 have been designated NONE. On the other hand, subset 1, to which all polytypes (including disordered regions) contribute, has been labeled ALL.

Table 1. *Distribution of reflections by indices and intensity*

Subset	Structure	Index conditions	Number of reflections	Number $> \sigma(I)$	$F_o^{\text{max}}$	$F_o^{\text{max}}/\sigma$
1	ALL	$h - k = 3n, l = 6n$	67	66	257	212
2	ABC	$h - k \neq 3n, l = 2n,$ $-h + k + l/2 = 3n$	94	88	214	250
3	ACB	$h - k \neq 3n, l = 2n,$ $h - k + l/2 = 3n$	94	41	24	70
4	AB	$h - k \neq 3n, l = 3n$	190	95	36	95
5	NONE	$h - k \neq 3n, l = 6n \pm 1$	190	34	10	20
6	NONE	$h - k = 3n, l \neq 6n$	339	33	8	7
	TOTAL	$h \geq 0, k \geq h, \pm l$	974	357		

Table 2. *Cell parameters*

	Data cell	3R	2H*
<i>a</i>	3.856 (1) Å	3.856 (1) Å	3.856 Å
<i>c</i>	32.905 (4)	16.453 (2)	10.968
<i>V</i>	423.7 (3) Å <sup>3</sup>	211.9 (2) Å <sup>3</sup>	141.2 Å <sup>3</sup>
<i>Z</i>	6	3	2
<i>F</i> (000)	348	174	116
<i>d</i> <sub>c</sub>	2.860 Mg m <sup>-3</sup>		

\* These numbers are derived from the refined cell parameters of a crystal that is primarily the 3R polytype. The actual cell parameters, especially *c*, for the 2H polytype may deviate somewhat from these values.

Parameters for the various cells are collected in Table 2. All calculations and results reported in this paper are based on the multiple cell used for data collection.

### 3. Structure determination and refinement

The solution of the structure and the recognition that polytypes were involved came from consideration of the strong subsets (1 and 2) of the data. For three CuNCS structural units in an *R* cell with Laue symmetry  $\bar{3}m$ , the only possible space group is *R3m* with atoms located in 3(*a*) on sites of  $3m$  symmetry. Thus, the CuNCS units must be linear and parallel, and the structure is composed of (001) layers of closest-packed cylinders of CuNCS units. Viewed end-on along [001], these layers look exactly like layers of closest-packed spheres. Just as in the polytypic stacking of layers of closest-packed spheres (Verma & Krishna, 1966), there are three possible layer positions in the *xy* plane. These correspond to placing atoms in turn on each of the threefold axes and are designated *A*, *B*, and *C*; the (*xy*) positions for atoms in *A*, *B*, and *C* are (00), ( $\frac{2}{3}\frac{1}{3}$ ), and ( $\frac{1}{3}\frac{2}{3}$ ), respectively.

The major portion of the crystal, therefore, corresponds to a 3R polytype (Zhdanov symbol  $\infty$ ) with the layer sequence *ABC*. The much weaker data of subset 3 result from the *R3m* reverse setting, which has a layer sequence *ACB*. The *ABC* and *ACB* structures differ only by a rotation of 60° around [001] and are really rotational twins. Subset 4 arises from a 2H polytype (Zhdanov symbol 11) with a layer sequence *AB*. Its space group must be *P6<sub>3</sub>mc* with atoms located in 3(*b*), again on sites of  $3m$  symmetry. Since the symmetry is hexagonal, the *hk* $\bar{l}$  reflections of subset 4 are redundant, although this is not obvious from the intensity data because of a relatively large anomalous-dispersion effect.

Equivalent positions for the doubled *R3m* cells and the tripled *P6<sub>3</sub>mc* cell are given in Table 3. To make the coordinates of the atoms in the asymmetric unit the same for each structure type, the origin for *P6<sub>3</sub>mc* was moved from the conventional location on  $6_3(3m)$  to one

of the other threefold axes. A trial set of atomic positions was obtained from the bond lengths of  $\alpha$ -CuNCS (Kabesova, Dunaj-Jurco, Serator, Gazo & Garaj, 1976). Since the space groups are polar, the Cu atom was fixed at (000) for the origin. Because of the  $3m$  site symmetry,  $B_{11} = B_{22} = 2B_{12}$  and  $B_{13} = B_{23} = 0$  for each atom. Thus, for refinement with anisotropic thermal parameters and an extinction correction, there are only 13 variable parameters.

Refinement was by full-matrix least squares which minimized  $\sum w(|F_o| - |F_c^*|)^2$  where  $F_c^* = KF_c(1 + gI_c)^{-1}$  in which *g* is an extinction parameter and *I<sub>c</sub>* is the calculated intensity. Weights were defined by  $w^{-1} = \sigma^2(F_o) + (0.02F_o)^2$ . Neutral-atom scattering factors were obtained from *International Tables for X-ray Crystallography* (1974). Corrections for anomalous scattering were applied for all atoms. The computer programs used were part of the Enraf-Nonius *Structure Determination Package* (1980) with some local modifications.

Initially, each of the structures was refined on the relevant data subset. The parameters of the *ABC* structure quickly converged and showed the necessity of an extinction correction. Refinement with the signs of the *z* parameters reversed showed conclusively that the correct polarity had been chosen. Isotropic thermal parameters had to be used in the *AB* and *ACB* refinements, since anisotropic thermal parameters did not refine satisfactorily. The positional parameters did not differ significantly for these three refinements.

The atomic parameters reported in Table 4 resulted from a refinement which utilized the 67 reflections (including 16 redundant *hkl*) of data set 1. The extinction factor refined to  $g = 0.99(6) \times 10^{-6}$ . The maximum parameter shift on the final cycle was 0.01 $\sigma$ , and the error of observation of unit weight was 0.95. The parameters did not differ significantly from those obtained previously with data subset 2 except for the scale factor, which is expected to be different (see

Table 3. *Equivalent positions*

<i>ABC</i>	<i>R3m</i> obverse	(000; $\frac{2}{3}\frac{1}{3}$ ; $\frac{1}{3}\frac{2}{3}$ ) + (00 <i>z</i> ; 00 $\frac{1}{2}$ + <i>z</i> )
<i>ACB</i>	<i>R3m</i> reverse	(000; $\frac{1}{3}\frac{2}{3}$ ; $\frac{2}{3}\frac{1}{3}$ ) + (00 <i>z</i> ; 00 $\frac{1}{2}$ + <i>z</i> )
<i>AB</i>	<i>P6<sub>3</sub>mc</i>	(000; $\frac{2}{3}\frac{1}{3}$ ) + (00 <i>z</i> ; 00 $\frac{1}{2}$ + <i>z</i> ; 00 $\frac{3}{2}$ + <i>z</i> )

Table 4. *Atomic parameters*

These parameters are relative to the expanded unit cell. The form of the anisotropic thermal parameter is

$$\exp \{-0.25[(h^2 + hk + k^2)a^{*2}B_{22} + l^2c^{*2}B_{33}]\}.$$

	<i>x</i>	<i>y</i>	<i>z</i>	<i>B</i> <sub>22</sub>	<i>B</i> <sub>33</sub>
Cu	0	0	0	2.69 (3) Å <sup>2</sup>	1.22 (2) Å <sup>2</sup>
N	0	0	0.05845 (17)	3.1 (3)	1.6 (2)
C	0	0	0.09337 (17)	1.4 (2)	1.9 (2)
S	0	0	0.14452 (4)	1.51 (5)	1.15 (4)

Table 5. *Agreement factors*

Subset	Structure	Reflections	<i>R</i>	<i>R<sub>w</sub></i>	<i>K(F<sub>o</sub>)</i>	<i>K<sub>i</sub><sup>2</sup>/K<sub>i</sub><sup>2</sup></i>
1	ALL	67	0.0163	0.0214	0.7025 (29)	1.000
1	ALL(- <i>z</i> )	67	0.068	0.102	0.742 (14)	
2	<i>ABC</i>	88	0.0183	0.0339	0.7539 (36)	0.868
3	<i>ACB</i>	41	0.093	0.068	7.382 (11)	0.009
4	<i>AB</i>	95	0.135	0.133	4.102 (14)	0.029

below). With these parameters held constant, the reflections with  $I > \sigma(I)$  in data subsets 2, 3, and 4, respectively, were used to refine only the scale factors for *ABC*, *ACB*, and *AB*. The agreement factors for these refinements and for a refinement of all the parameters of the structure with *z* reversed are given in Table 5.\*

For each of data subsets 1–4, the refined scale factor is expected to be different because a different quantity of material contributed to the intensities in each case. In particular, ratios of the squares of the scale factors are quantitative measures of the polytypic composition of the crystal investigated. Shown in Table 5 are the scale factors and the ratios  $K_i^2/K_j^2$ , which show that the data crystal is a coalescence of 87% *ABC*, 1% *ACB*, 3% *AB*, and 9% OTHER. The OTHER category, determined by difference, contains any higher polytypes that may be present and also the disordered regions. The original crystal investigated appeared to contain no *ACB* but a considerable amount of *AB*.

## Results

The crystal structure, based on the stacking of (001) layers of closest-packed CuNCS cylinders, has already been detailed above, since the analysis of the data required an understanding of the composition of the crystal. Adjacent layers are strongly bonded to each other at each Cu and S atom by three equivalent Cu–S bonds such that both Cu and S are tetrahedrally coordinated and the crystal is a giant three-dimensional polymeric molecule. The Cu–S bonds at opposite ends of a cylinder are staggered in the 3*R* polytype and eclipsed in the 2*H* polytype. A stereoscopic view (Johnson, 1971) of the 3*R* structure is shown in Fig. 2.

Bond lengths and angles are given in Table 6 and compared with similar quantities in  $\alpha$ -CuNCS (Kabesova, Dunaj-Jurco, Serator, Gazo & Garaj, 1976) and in  $C_6H_5N^+.[Cu_2(SCN)_3]^-$  (Raston, Walter & White, 1979). The bond lengths agree very well for the three compounds; however, very significant differences are apparent in the angles. High site symmetry in  $\beta$ -CuNCS causes the angles to be very regular. The

N–C–S and Cu–N–C sequences are strictly linear, and the two independent angles at Cu and S are very nearly tetrahedral ( $109.5^\circ$ ). The  $\alpha$ -CuNCS and  $[Cu_2(SCN)_3]^-$  structures are not symmetry constrained, and the angles show a wide divergence from equivalence and from ideal values. The N–C and C–S distances and N–C–S angle in  $\beta$ -CuNCS also agree exceptionally well with the values 1.149 (15), 1.689 (13) Å, and  $178.3 (1.2)^\circ$ , respectively, found in KNCS (Akers, Peterson & Willett, 1968).

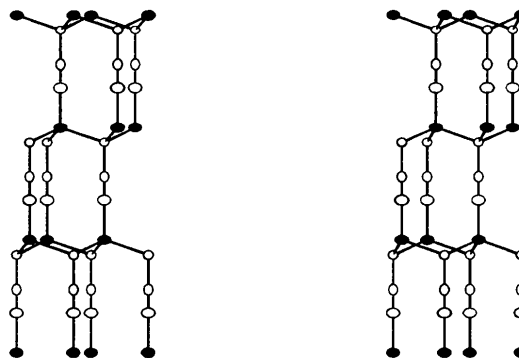


Fig. 2. Stereoscopic view of the 3*R* polytype. The filled atoms are Cu. The vertical axis is *c* and  $[3\bar{1}0]$  is horizontal, left to right. The atoms are represented by 50% probability thermal ellipsoids.

Table 6. *Bond lengths (Å) and angles (°)*

	$\beta$ -CuNCS <sup>(a)</sup>	$\alpha$ -CuNCS <sup>(b)</sup>	$[Cu_2(SCN)_3]^-$ <sup>(c)</sup>
Cu–S	2.343 (1)	2.344 (2)	2.319 (3)
		2.354 (2)	2.421 (3)
		2.367 (2)	2.448 (3)
Cu–N	1.923 (11)	1.927 (6)	1.926 (9)
		1.149 (15)	1.15 (1)
N–C	1.149 (15)	1.116 (9)	1.15 (1)
			1.15 (1)
C–S	1.683 (9)		1.14 (1)
			1.63 (1)
			1.66 (1)
N–C–S	180	1.696 (7)	1.66 (1)
			178.5 (9)
			176.6 (9)
Cu–N–C	180	178.7 (7)	178.6 (10)
			165.7 (8)
			108.6 (1)
S–Cu–S	110.78 (5)	103.01 (7)	107.1 (1)
		107.28 (7)	103.7 (1)
		110.15 (7)	103.7 (1)
N–Cu–S	108.13 (5)	115.0 (2)	120.4 (3)
		114.4 (2)	110.0 (3)
		106.3 (2)	106.4 (3)
Cu–S–Cu	110.78 (5)	129.9	
		111.4	( <i>d</i> )
		99.8	
Cu–S–C	108.13 (5)	104.9	
		104.7	( <i>d</i> )
		103.4	

\* Lists of structure factors for data subsets 1–4 have been deposited with the British Library Lending Division as Supplementary Publication No. SUP 36098 (7 pp.). Copies may be obtained through The Executive Secretary, International Union of Crystallography, 5 Abbey Square, Chester CH1 2HU, England.

Notes: (*a*) This study. (*b*) Kabesova, Dunaj-Jurco, Serator, Gazo & Garaj (1976). (*c*) Raston, Walter & White (1979). (*d*) S in this structure is pyramidal rather than tetrahedral. Lone-pair repulsion causes considerable reductions in the angles at S.

The crystals of  $\beta$ -CuNCS are polar, and all of the CuNCS cylinders point in the same direction. By direct observation of the crystal orientation on the diffractometer, we determined that the apex of the crystal represents the +*c* direction. Therefore, the S ends of all cylinders point toward the apex and, conversely, the Cu ends of all cylinders point toward the base of the trigonal-pyramidal crystals. The space-group symmetry requires that atoms of one type lie rigorously in planes parallel to (001). Planes containing Cu atoms lie 0.73 Å from planes containing S atoms and form laterally bonded bands of (CuS)<sub>n</sub> perpendicular to *c*. These bands are interlinked along *c* by the NC groups. In the centrosymmetric  $\alpha$ -CuNCS crystals, the slightly bent CuNCS groups zigzag in both directions along *a*; the Cu and S atoms, however, also lie in narrow bands which are also interlinked by NC groups. In this case, the bands are perpendicular to *a*, are slightly undulatory along *b*, and are of somewhat greater width. It is noteworthy that the lattice constants in the chain directions differ by only  $3\sigma$  [ $c_\beta/3 = 10.968$  (1),  $a_\alpha = 10.994$  (9) Å]. Apparently, the tilt and bends of the CuNCS units in  $\alpha$ -CuNCS are compensated by the slightly longer Cu–S bonds. The slight staggering of the CuNCS units in the  $\alpha$  form allows a closer lateral packing, which results in the  $\alpha$  form being denser ( $d_c = 3.05$  Mg m<sup>-3</sup>) than the  $\beta$  form ( $d_c = 2.86$  Mg m<sup>-3</sup>).

The polytypism of  $\beta$ -CuNCS based on closest packing of cylinders is apparently unique, but nevertheless has close parallels in other materials such as C, ZnS, and SiC which also exhibit tetrahedral bonding. For example, the ABC structure resembles that of ordinary diamond if one considers two adjacent C atoms to describe a cylinder. Likewise, in cubic ZnS (zinc blende or sphalerite) or in  $\beta$ -SiC, one can consider ZnS or SiC units as cylinders. By expanding the cell along the cylinder axis, one would change the cell symmetry from cubic 3C to rhombohedral 3R. Actually, a 3R form of ZnS ( $\gamma$ -ZnS) was once reported (Buck & Stroock, 1955). The 2H or AB polytype also exists in SiC and ZnS (wurtzite). Even without expansion into cylinders, the symmetry ( $P6_3/mc$ ) is the

same. Therefore, one could consider the polytypes of  $\beta$ -CuNCS to be isostructural with the polytypes of ZnS and SiC and with the numerous other compounds that have close-packed layer structures with tetrahedral bonding (Wyckoff, 1963).

We thank Dr R. P. Scaringe for helpful discussions concerning the crystallography of polytypes and Dr D. S. Bailey for assistance with the IR analyses.

#### References

- AKERS, C., PETERSON, S. W. & WILLETT, R. D. (1968). *Acta Cryst.* B24, 1125–1126.
- BUCK, D. C. & STROCK, L. W. (1955). *Am. Mineral.* 40, 192–200.
- GARAJ, J. & GAZO, J. (1965). *Chem. Zvesti.* 19, 593–603.
- International Tables for X-ray Crystallography* (1974). Vol. IV, ch. 2. Birmingham: Kynoch Press.
- JCPDS (1979). *Powder Diffraction File*, Vol. 29, pp. 581, 582.
- JOHNSON, C. K. (1971). ORTEP II. Report ORNL-3794, second revision. Oak Ridge National Laboratory, Tennessee.
- KABESOVA, M., DUNAJ-JURCO, M., SERATOR, M., GAZO, J. & GARAJ, J. (1976). *Inorg. Chim. Acta*, 17, 161–165.
- KABESOVA, M., KOHOUT, J. & GAZO, J. (1978). *Inorg. Chim. Acta*, 31, L435–L436.
- KRUGER, D., BUSSEM, W. & TSCHIRCH, E. (1936). *Chem. Ber.* 69, 1601–1610.
- KRUGER, D. & TSCHIRCH, E. (1941). *Chem. Ber.* 74, 1378–1386.
- NORTH, A. C. T., PHILLIPS, D. C. & MATHEWS, F. S. (1968). *Acta Cryst.* A24, 351–359.
- RASTON, C. L., WALTER, B. & WHITE, A. H. (1979). *Aust. J. Chem.* 32, 2757–2761.
- Structure Determination Package* (1980). Revision 3B. Delft: Enraf–Nonius.
- TRAMER, A. (1962). *J. Chim. Phys. Chim. Biol.* 59, 232–240.
- VERMA, A. R. & KRISHNA, P. (1966). *Polymorphism and Polytypism in Crystals*. New York: John Wiley.
- WYCKOFF, R. W. G. (1963). *Crystal Structures*, 2nd ed., Vol. 1, p. 110. New York: Wiley–Interscience.